Chemical Imaging using Infrared Photo-thermal Microspectroscopy

Robert Furstenberg*, Christopher A. Kendziora, Michael R. Papantonakis, Viet Nguyen and R. A. McGill
U.S. Naval Research Laboratory, Code 6365, 4555 Overlook Ave SW, Washington, DC 20375, USA

ABSTRACT

There is a growing need for new characterization techniques that can provide information about the chemical composition of surfaces and bulk materials with spatial resolution in the range of 1-10 microns. While FTIR micro-spectroscopy addresses this problem, the practical resolution limit is still only about 20 microns. Other well-established techniques at the nanometer are impractical at the micro-scale. Raman micro-spectroscopy provides adequate spatial resolution (~1 micron), but may not always be useful due to its low throughput and for samples with strong fluorescence. We are developing a non-contact and non-destructive technique that provides similar information as IR or Raman spectroscopy. It involves photo-thermal heating of the sample with a tunable quantum cascade laser (or other suitable infrared laser) and measuring the resulting increase in thermal emission by either an infrared detector or a laser probe in the visible spectral range. The latter case allows for further increase of the spatial resolution from ~10 microns to ~1 micron, at the right experimental conditions. Since the thermal emission signal from the surface is directly proportional to the absorption coefficient, by tuning the laser wavelength we directly measure the IR spectrum of the sample. By raster-scanning over the surface of the sample we can obtain chemical composition maps. We demonstrate this technique by imaging the surface of several different materials. We analyze the spatial resolution of our photo-thermal imaging system as well as discuss the conditions under which the spatial resolution can be further increased from the infrared far-field diffraction limit.

Keywords: Microspectroscopy, infrared, quantum cascade laser, QCL, photo-thermal, characterization, chemical imaging, hyperspectral

1. INTRODUCTION

Currently, there are several characterization techniques for chemical imaging of samples with a wide range of achievable spatial resolution. However, these techniques are not always well suited for samples where the required spatial resolution is 0.1 - ~1 microns. For example, FTIR spectroscopy provides the chemical composition but without spatial information. While FTIR micro-spectroscopy addresses this problem, the practical resolution limit is limited to about ~20 μm (in the mid-infrared or fingerprint region from ~5-12microns). X-Ray mapping can achieve much higher resolution but provides elemental maps, though this is not very useful for the identification of organic compounds. On the other hand, well-developed imaging techniques at the nanometer scale (scanning probe microscopy (SPM), atomic force microscopy (AFM), transmission electron microscopy (TEM) and its variant TEM/EELS etc.) may be impractical at the micron-scale due to small scanning speeds and limited scan range and more importantly because they provide limited chemical information about the sample. The emerging technique of Raman micro-spectroscopy provides adequate spatial resolution (~1 μm), but may not always be useful due to its low throughput and in cases where strong fluorescence suppresses the weak Raman signature. Another promising AFM-based technique, now available as a commercial instrument (nano-IR by Anasys Inc.) can achieve spatial resolution of ~100nm but requires very thin microtomed samples. Therefore, it appears that there is room for more new chemical imaging techniques, especially ones that require no sample preparation and can be performed in a non-contact and non-destructive manner.

In this paper we present a novel chemical imaging technique based on infrared photo-therrmal spectroscopy that has the potential to generate chemical images of samples with a spatial resolution of ~1um (below the far-field diffraction limit of a mid-IR beam).

*Email: robert.furstenberg@nrl.navy.mil; Phone: 202-767-5947

Next-Generation Spectroscopic Technologies V, edited by Mark A. Druy, Richard A. Crocombe,
Proc. of SPIE Vol. 8374, 837411 · © 2012 SPIE · CCC code: 0277-786X/12/$18 · doi: 10.1117/12.919574

Photo-thermal spectroscopy (PTS) involves periodic heating of the sample and monitoring its response using either an IR detector or a visible probe beam (usually a HeNe laser) [1]. The photo-thermal signal is proportional to the absorption coefficient and the PT spectra resemble FTIR absorbance spectra, as illustrated in Figure **1**. We have already successfully applied our PTS implementation, photo-thermal IR imaging spectroscopy (PT-IRIS) for detection of chemicals at a distance [2]. In PT-IRIS, we use quantum cascade lasers (QCLs) to heat the sample and a long-wave IR detector as the imager. By tuning the QCL across characteristic absorption bands we map out the chemical composition of the sample. In this paper, we describe a modified instrument suitable for microscopy application.

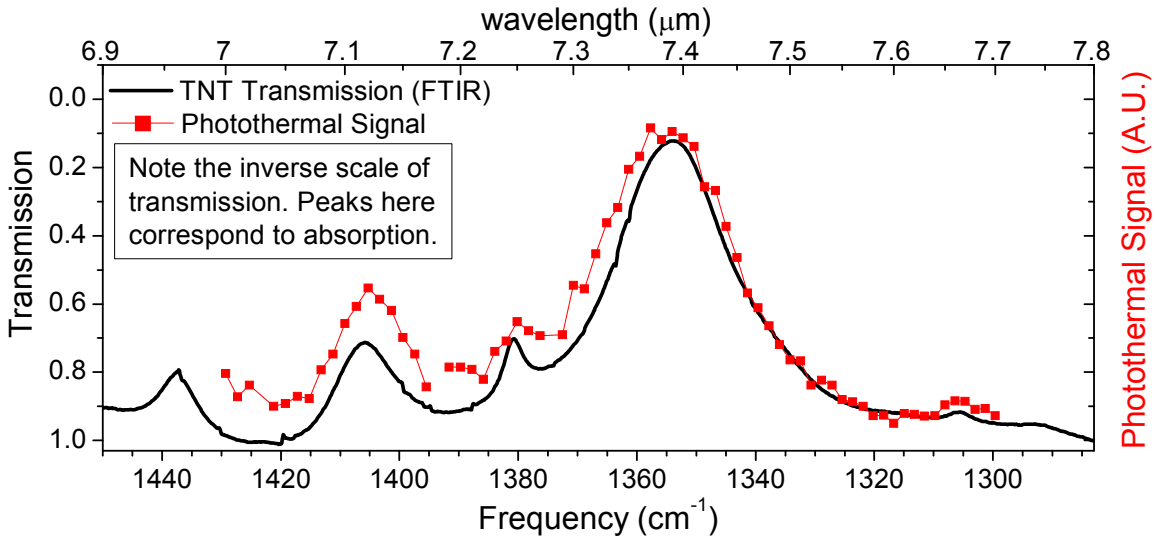

Figure 1. Comparison of the photo-thermal signal with FTIR transmission data.

2. EXPERIMENTAL DETAILS

2.1 Photo-thermal confocal microscope

Figure 1 shows the schematic drawing of the PT-IRIS microscope. The infrared light from a tunable QCL (Daylight Solutions Inc.) is combined with the output from a laser diode (~650nm) using a dichroic filter. Both beams are focused on the sample using a reflecting objective (25X, 0.4NA). The sample rests horizontally on a motorized stage. The visible light reflected from the sample is focused onto a multi-mode optical fiber (100 μm core size) which carries the light to an avalanche photo-diode. Since using the 100 μm core size would unnecessarily degrade the spatial resolution, we placed a 25 μm pinhole before the fiber. The focusing of the laser beam on the sample is achieved by inserting a removable viewer in the beam path before the objective. The viewer is equipped with a beamsplitter that directs the reflected beam to a camera.

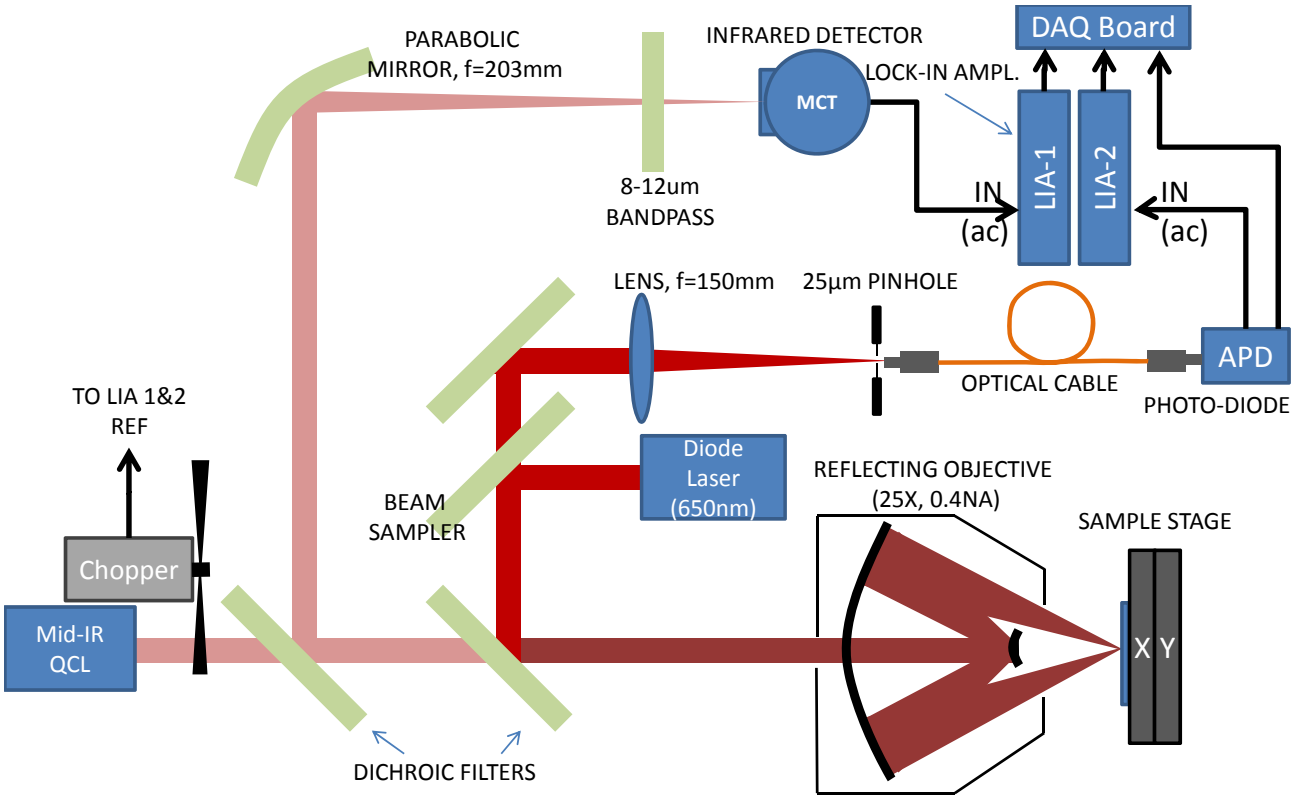

Figure 2. Schematic drawing of the photo-thermal confocal microscope.

The IR photo-thermal signal is collected with the same objective and focused onto a single channel IR detector (IR Associates, MCT-13-0.50) which has a 500 µm detector element. With this approach, the photo-thermal effect can be detected by two different probes (visible and IR). The IR laser is modulated (50% duty cycle) using a mechanical chopper. Both the visible probe and IR detector signals are demodulated using a digital lock-in amplifier. The DAQ board also collects the dc-component of the photo-diode signal as in a conventional confocal microscope. A custom data acquisition and visualization software program was written. By removing the 8-12 µm bandpass filter and replacing the dichroic filter (closest to the laser) with a beam splitter, the setup is easily converted to measure IR reflectance.

2.2 Spatial resolution

The spatial resolution of the IR detector probe is diffraction limited. The theoretical laser spot size is given by [3,4]

$$D_{spot} = \frac{4M^2\lambda f}{\pi D_{laser}} \quad (1)$$

For the test-bed shown in Figure 1 and for λ=6.25 µm, M^2=1.3 (manufacturer's claim), D_{laser}=7 mm (measured using a beam profiler) and f=6.4 mm the laser spot is D_{spot} =9.5 µm.

The spatial resolution of the visible probe has an upper limit given by the diffraction limit of the visible light which, for a 0.4NA objective, is slightly larger than the wavelength of light. This means that under certain conditions, photo-thermal microscopy can achieve 1 µm or even sub-micron resolution. In our test-bed, the optics are chosen for a ~>1 µm limit, which is adequate given the use of a multimode laser diode which cannot focus to a smaller spot. PTS spatial resolution is driven by the thermal diffusivity of the sample. In order to take full advantage of the spatial resolution of the visible

probe, the IR excitation laser needs to be modulated at a high enough frequency in order to limit thermal diffusion. This frequency (f_{mod}) is a function of not only sample diffusivity but also geometry. The worst-case value for the spatial resolution is given by the thermal diffusion length [5]

$$\Delta L=(4\alpha/f_{mod})^{0.5} \quad (2)$$

Where α is the thermal diffusivity of the sample. For particular samples consisting of mixtures and particulates on surfaces where the thermal coupling in weaker, the thermal diffusion length is much small than the one given by Eq. 2.

2.3 Diffraction-limited photo-tehermal microscope

In this modality, the spatial resolution is diffraction limited, just like in FTIR micros-spectroscopy. Even so, the the use of bright lasers (as opposed to dimmer incoherent sources) in a confocal geometry and the ability to acquire absorbance-like data in reflection offer several potential advantages over traditional FTIR micro-spectroscopy. Also, in addition to the photo-thermal signal (proportional to the absorption coefficient) we can also measure reflectance by simply replacing the dichroich filter that separates the excitation laser wavelengths from the collection wavelengths by a beamsplitter. Figure 3 shows the schematic of the diffraction limited photo-thermal microscope.

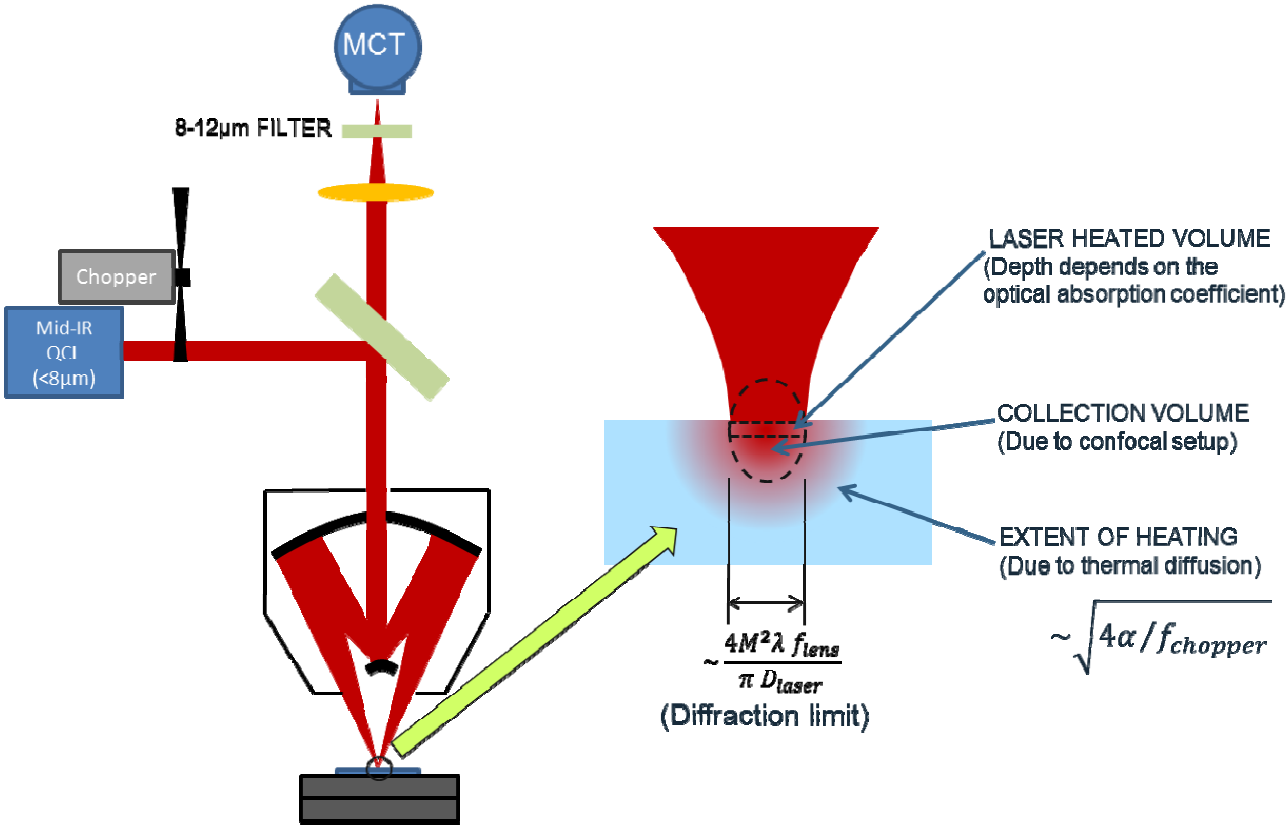

Figure 3. Schematic drawing of the diffraction-limited photo-tehrmal microscope mode.

2.4 Sensing with the confocal visible probe (sub-diffraction limited mode)

Along with measuring the thermal emission (as described in the previous section), the photo-thermal effect can also be sensed by a visible laser probe that utilizes two phenomena that occur during the laser/sample interaction:

Thermo-optic effect

The thermo-optic effect is manifested in the periodic change in reflectance from the sample-air interface due to the periodic heating of the sample and air (through heat transfer from sample) and subsequent change in their refractive indices.

The reflectance coefficient at the sample-air interface is given by [6]

$$R = \left(\frac{n_s - n_a}{n_s + n_a}\right)^2 \tag{4}$$

A thermally induced change in the indices of refraction will result in a change in reflectance given by

$$\frac{\Delta R}{R} = 4\frac{n_a\frac{\partial n_s}{\partial T} - n_s\frac{\partial n_a}{\partial T}}{n_s^2 - n_a^2}\Delta T \tag{5}$$

where $\frac{\partial n_s}{\partial T}$ and $\frac{\partial n_a}{\partial T}$ are the thermo-optic coefficients for the sample and air, respectively.

Thermo-elastic effect

The thermo-elastic effect is based on the fact that the sample expands thermally in response to each IR laser pulse, thus modulating the sample position to which the confocal setup is sensitive; When heated, the focused laser spot on the sample becomes slightly out of focus and the photodiode is collecting less light. The beam radius away from a focused spot ($z \neq 0$) is given by [3]

$$w^2(z) = w_0^2\left[1 + \left(\frac{\lambda z}{\pi w_0^2}\right)^2\right] \tag{6}$$

where w_0 is the beam waist radius at focus, λ the laser wavelength, and z the distance from the focal spot along the optical axis. If the surface of the sample bulges up (due to heating) by

$$\Delta z = \beta \Delta T \tag{7}$$

where β is the thermo-elastic coefficient, then the change in collected signal at the confocal aperture (or fiber optic input) of the photo-diode is

$$\frac{\Delta I}{I} = -\left(\frac{\lambda^2\beta^4}{\pi^2 w_0^4}\right)\Delta T^2 \tag{8}$$

The relative contribution of each of these mechanisms will depend on the thermo-optic and thermal expansion coefficients for the given sample. Both of these signals are weak and require a light detector with very high sensitivity. In this work we used avalanche photo-diodes but there were not sensitive enough for all samples. A photo multiplier tube would be a better choice. Figure **4** shows the schematic of the sub-diffraction limited photo-thermal microscope.

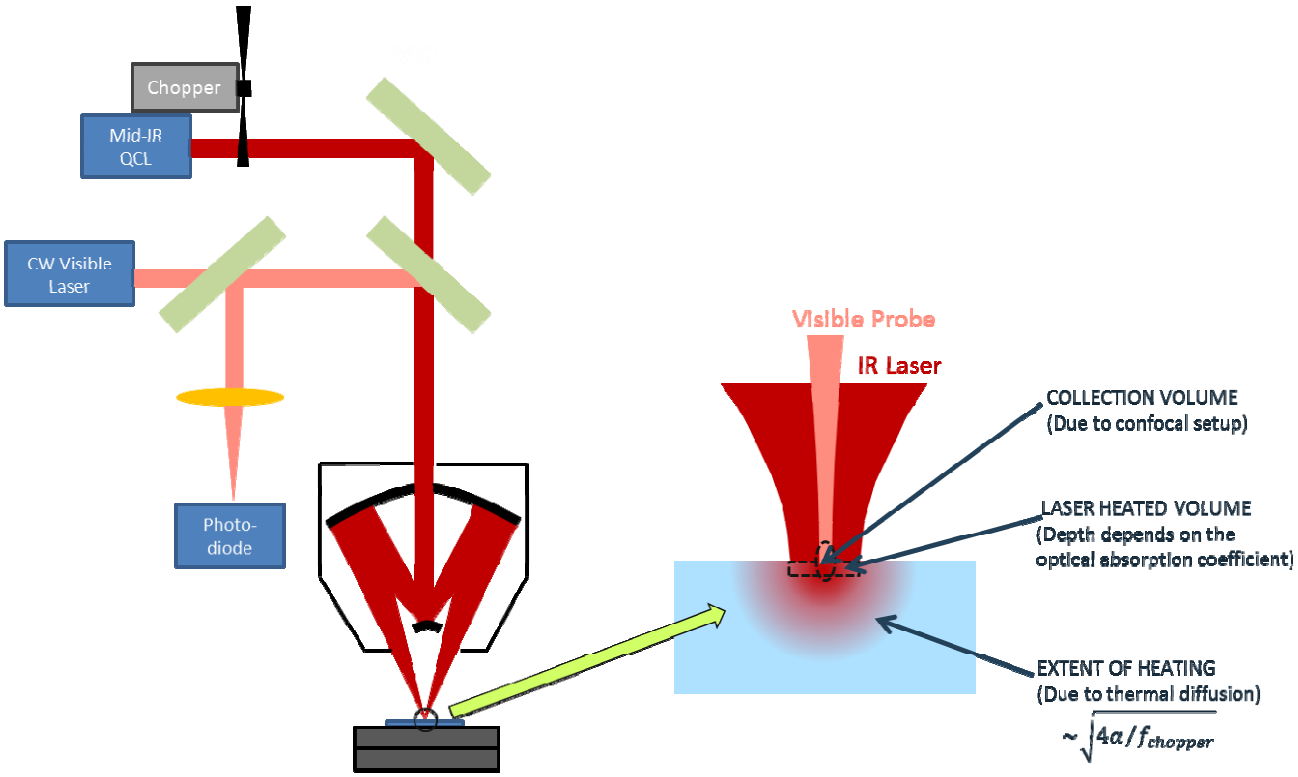

Figure 4. Schematic drawing of the sub-diffraction-limited photo-tehrmal microscope mode.

2.5 Test samples

In this paper, we study 3 different test samples:

1. A microscope calibration slide. It provides a sharp transition region from a thin metallic coating to bare glass which is useful in testing the spatial resolution of the microscope.

2. A crystal of 2,6-dinitrotoluene (DNT) on a glass slide. The sample was prepared by placing a crystal of DNT between two glass slides and applying pressure to crush in into smaller sized crystals.

3. A MEMS chemical vapor preconcentrator consisting of a thin perforated polyimide membrane supported by a silicon frame. The membrane has platinum meander-trace wires for heating and temperature sensing and is shown in Figure **5**. [7]

We examined two versions: uncoated and one coated with a thin layer (0.9 μm) of a hydrogen-bond acidic hyperbranched carbosilane sorbent polymer (HCSFA2) used for selective adsorption of explosive vapors [8]. A 5% solution of HCSFA2 in butanol was deposited on the device by an ink-jetting instrument (JetlabII by Microfab Inc).

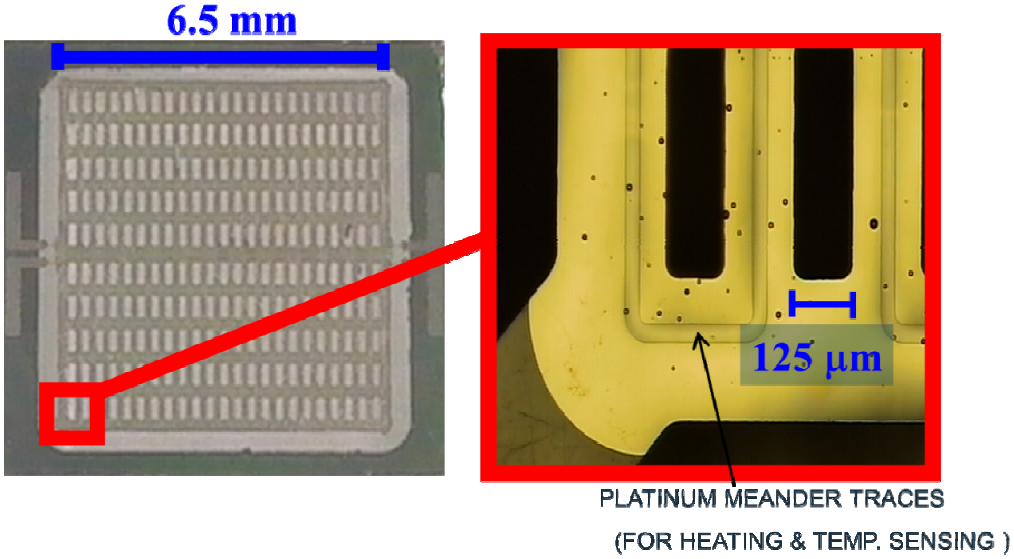

Figure 5. Optical micrographs of the Cascade Avalanche Sorbent Plate Array (CASPAR), a MEMS chemical vapor preconcentrator.

3. DISCUSSION

3.1 Spatial resolution test using the calibration slide

To test the intrinsic spatial resolution of the visible probe, we performed a line scan of the laser spot over the metal/glass edge. The results are shown in black lines with open triangles in Figures 2a-c and the spatial resolution is estimated to be 1-2 µm (in line with the 1 µm theoretical limit for the given test-bed). To test the resolution of the IR probe, we scanned the focused IR laser beam over the same edge and monitored the reflected IR signal. Figure 2b indicates that the resolution is approximately 10 µm.

We were also able to observe the photo-thermal effect by using both probes. The result of the line scan for the IR probe is shown in Figure 2b and for the visible probe in Figure 2c. However, it should be pointed out that this slide, (due to large contrast in reflectance) is not a suitable test sample to ascertain the spatial resolution for the photo-thermal probes. With this caveat, the resolution appears to be ~10 µm in Figure 2b and 2 µm in Figure 2c. Test samples studied in the next two subsections provide further clues about the spatial resolution of the microscope.

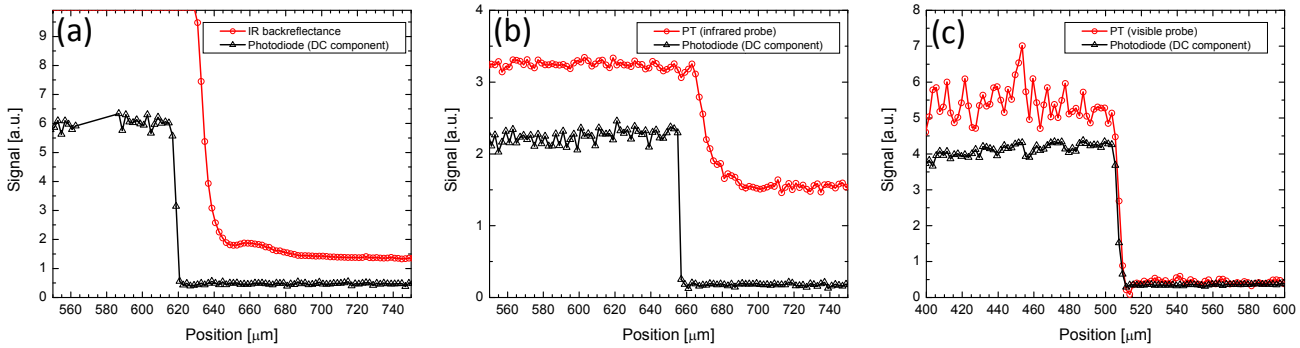

Figure 6. Line scans across a sharp metal/glass interface of a calibration slide. Open triangles correspond to the dc component of the visible probe. Open circles correspond to the IR back-reflectance (a), IR PT signal (b) and visible PT probe signal (c).

3.2 Chemical imaging of a small crystal

To examine the chemical imaging capability of the PT microscope, we imaged a crystal of DNT on a glass slide. Both the DNT and glass absorb the IR laser and subsequently produce a photo-thermal response so this is a challenging test sample for imaging.

The spatial raster scan consisted of 12 by 12 points with a 15 μm step size. The laser was tuned to 35 discrete wavelengths in the 6-6.6 μm spectral region. The raster scan was repeated for each wavelength. The dwell time at each point was ~300 ms, which was the minimum time required to move the stage between points. Figure 3a shows the optical image of the crystal, while Figure 3b shows the confocal microscope image. Figures 3c to 3e show images generated by the PT IR probe with the laser tuned to three different wavelengths. The wavelength in the last image (Figure 3e) is near the absorption peak of DNT.

Due to the lack of flatness of the sample, we were only able to observe the photo-thermal signal for the IR probe as the visible light probe has a significantly smaller depth of focus (~1 μm vs. ~10 μm for IR probe) and was defocused when on the crystal. The intensity of reflected light was below the noise level of the photo-diode. Another contributing factor was the lower amount of laser power (~4 mW) used to prevent the crystal from melting (T_m=66°C).

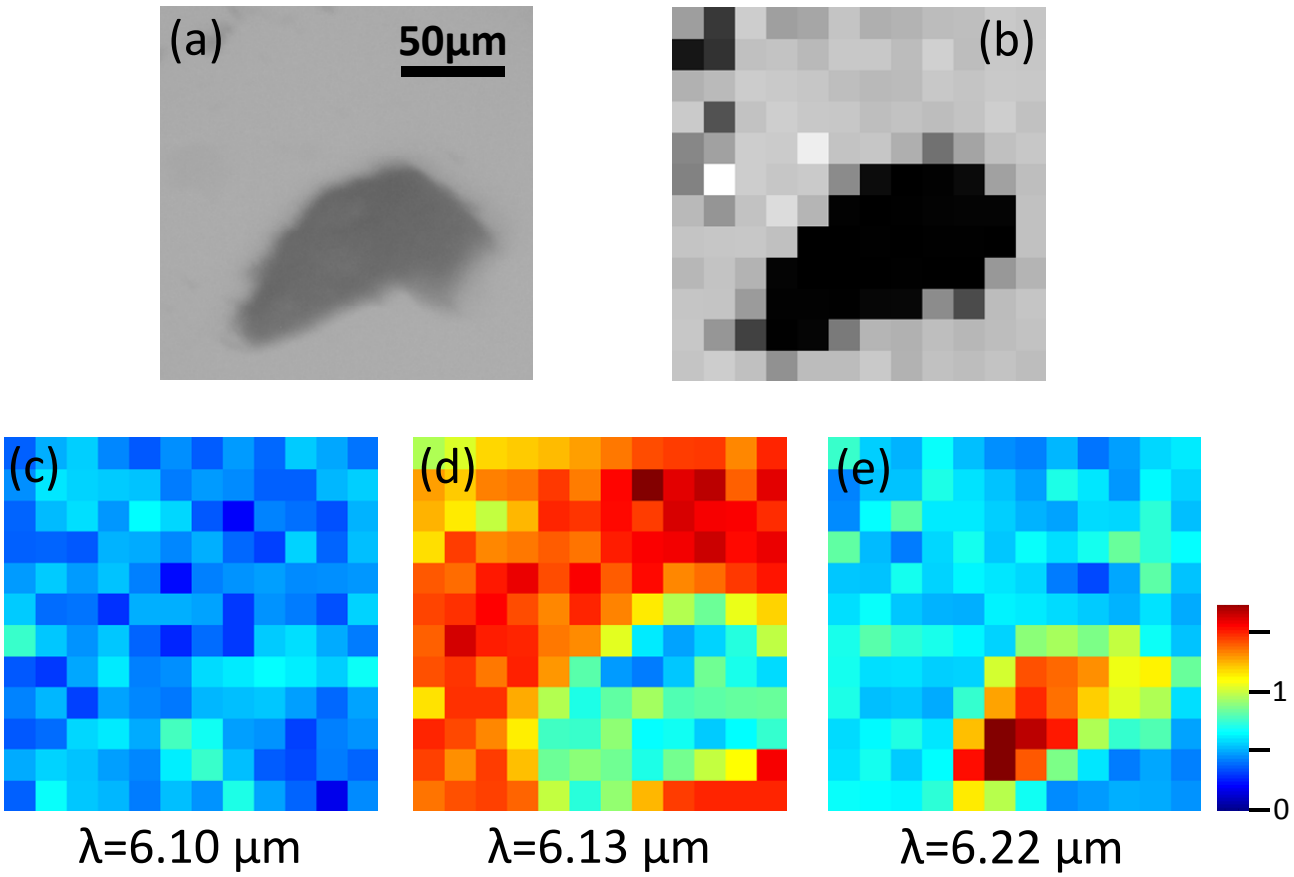

Figure 7. Photo-thermal imaging of a DNT crystal on glass.

3.3 Chemical imaging of a MEMS device

As a third test we image a portion of the sorbent polymer coated MEMS preconcentrator device as shown in Figure 4a. The spatial raster scan consisted of 25 by 25 points with 12 µm steps. The laser was tuned to 14 discrete wavelengths in the 6-6.6 µm spectral region. The polyimide membrane and the HCSFA2 sorbent coating have absorption features that peak at 6.17 µm and 6.30 µm respectively, and are mapped in Figures 4c and 4d. The polyimide spectrum from an uncoated device is shown in Figure 4e. The PT spectrum on top of the platinum trace (Figure 4f) matches that of pure HCSFA2. In other parts of the device, the spectra are mixtures of polyimide and HCSFA2, as shown in Figure 4g. A suitable chemometrics algorithm could be used easily determine the

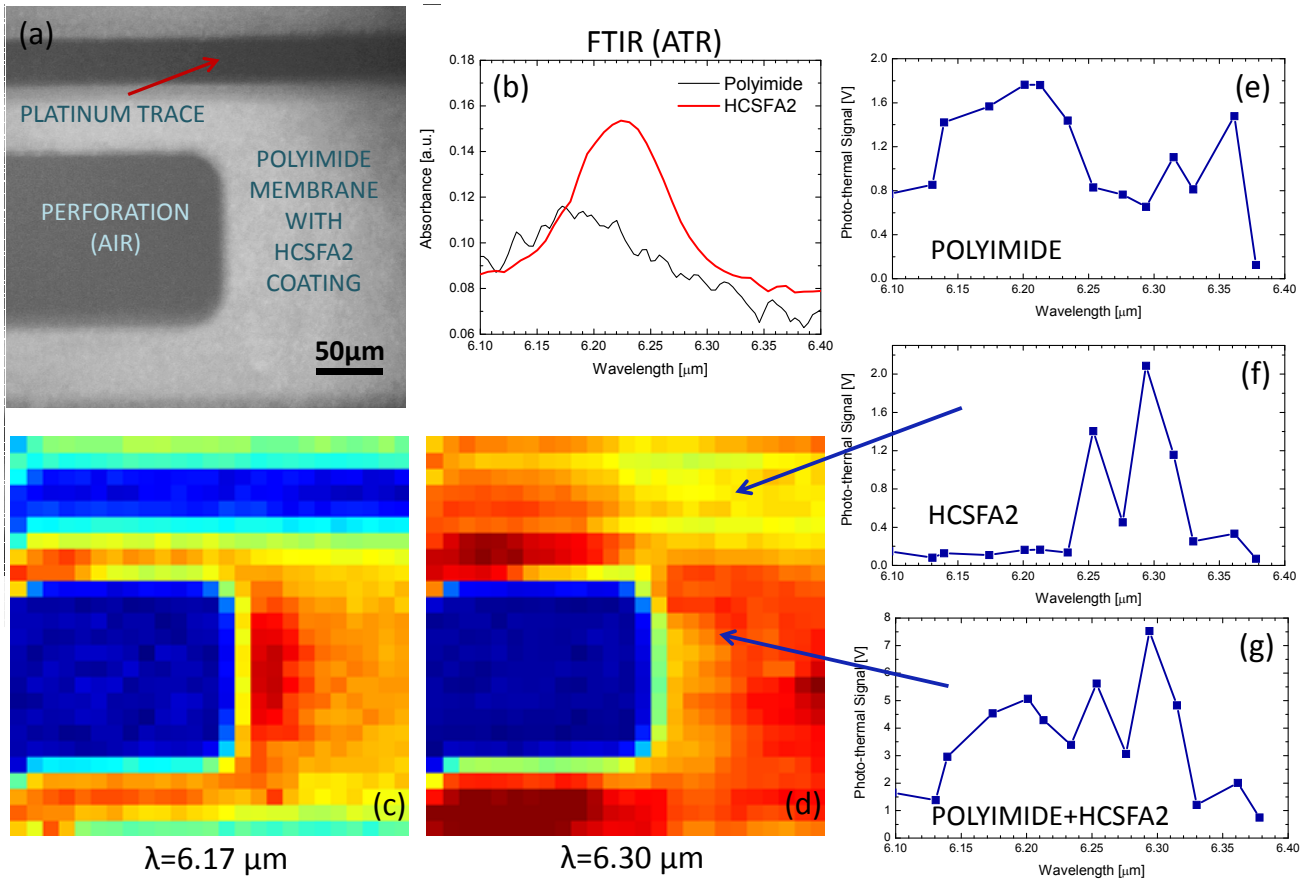

Figure 8. Chemical imaging of a MEMS preconcentrator coated with a sorbent polymer.

4. CONCLUSIONS

We designed and built a photo-thermal microscope capable of chemical imaging with a resolution of ~10 μm. By using a visible light probe, this resolution can be further increased. However, we found that the visible probe signal is weak for certain samples and requires the samples to be flat. A better photo-diode and/or an interferometry-based light detection scheme will be used in the future to improve the photo-thermal signal strength.

We demonstrated our microscope on various test-samples. We were able to chemically image an organic crystal on a complex, IR-absorbing substrate. We also used the microscope to image the IR spectra of a sorbent polymer coated MEMS device. We showed that the coating process was successful and that the device surface was fully coated, with some thickness variation.

5. ACKNOWLEDGMENTS

This research was supported by funding from ONR/NRL.

REFERENCES

[1] Sell, J. A., [Photo-thermal Investigations of Solids and Fluids], Academic Press Inc., San Diego, 1-30 (1988).
[2] Furstenberg, R., Kendziora, C. A., Stepnowski, J., Stepnowski, S. V., Rake, M., Papantonakis, M. R., Nguyen, V., Hubler, G. H., and McGill, R.A., "Stand-off detection of trace explosives via resonant infrared photothermal imaging", Appl. Phys. Lett., 93, 224103 (2008).
[3] Young, M., [Optics and Lasers, 5th Ed.], Springer-Verlag, Berlin & Heidelberg & New York, 243 (2000).
[4] Sun, H., "Thin lens equation for a real laser beam with weak lens aperture truncation", Opt. Eng., 37(11) 2906–2913 (1998).
[5] Carslaw, H. S., Jaeger, J. C., [Conduction of heat in solids], Clarendon Press, Oxford (1959)
[6] Young, M., [Optics and Lasers, 5th Ed.], Springer-Verlag, Berlin & Heidelberg & New York, 221 (2000).
[7] Martin, M., Crain, M., Walsh, K., McGill, R. A., Houser, E., Stepnowski, J., Stepnowski, S. V., Wu, H. D. and Ross, S., "Microfabricated vapor preconcentrator for portable ion mobility spectroscopy", Sensors And Actuators B - Chemical 126, 447-454 (2007).
[8] Higgins, B. A., Simonson, D. L., Houser, E. J., Kohl J. G. and McGill, R. A., "Synthesis and Characterization of a Hyperbranched Hydrogen Bond Acidic Carbosilane Sorbent Polymer", J. Pol. Sci. Part A. 48, 3000-3009 (2010) .